Formation of Diamond-Like Carbon Films by Plasma-Based Ion Implantation and Their Characterization

Wolfgang Ensinger[*]

Department of Materials Science, Chemical Analytics, Darmstadt University of Technology
Petersenstr. 23, 64287 Darmstadt, Germany

Plasma-based ion implantation (PBII) allows the formation of diamond-like carbon (DLC) films with excellent tribological properties. A large number of examples from the literature are discussed in detail, and the process parameters of PBII, such as plasma-forming gas, bias voltage, pulse length, pulse repetition rate and experimental setup, are correlated with the DLC film properties, such as bonding characteristics, stress, hardness, friction and wear behavior and corrosion protection ability. Trends in the variation of film features with the process parameters are shown, and the underlying physical processes are discussed.

1.   Introduction

Diamond-like carbon (DLC) films have a considerable content of sp^3 carbon bonds (diamond bonds). Their C-C bond lengths are of regular dimension; however, the bond angles often deviate from those of C-C bonds, found at the diamond tetraeder. Therefore, they are more or less amorphous. For this reason, they belong to the class of amorphous carbon films (a-C). When they are formed from hydrocarbons, they contain a certain amount of hydrogen. This is why they are abbreviated as a-C:H. DLC films are smooth and hard but comparatively elastic, have a low friction coefficient, and a low intrinsic microporosity, while they are chemically highly stable against different media. For these reasons, they are excellently suitable as thin protective films both for mechanical or tribological protection (against wear) and chemical protection (against corrosion). An example is the application

[*]Corresponding author: e-mail: ensinger@ca.tu-darmstadt.de

as a tribologically and corrosion-protective film for magnetic recording heads, used in every personal computer. Other applications are cutting tools, machining tools, orthopedic devices, textile manufacturing components, and engine components. Further favorable features of DLC films are high optical transparency, high thermal conductivity, and good field emission properties. These features make them suitable for a number of applications in microelectronics or optics.

DLC films have been deposited by a number of techniques with energetic ions involved. The ions are responsible for the phase formation and structure of the films. Several effects may play a role such as stress-induced phase transition or subplantation. The ions are gained either from an ion beam, such as in ion beam deposition (IBD) and ion-beam-assisted deposition (IBAD), or from a plasma such as in plasma-enhanced chemical vapor deposition (PE-CVD) or in cathodic vacuum arc deposition (CVAD). In the last two decades, another method has been used for depositing DLC films, namely, plasma-based ion implantation PBII,[1] also termed plasma immersion ion implantation PIII or plasma source ion implantation PSII.[2] When the aspect of film deposition is stressed, it is called plasma immersion ion implantation and deposition (PIIIaD), or simply plasma immersion ion deposition (PIID).

Figure 1 shows a simple sketch of a typical PBII setup. It consists of a vacuum chamber, a gas supply system, a plasma generator, and an insulated sample holder, connected to a high-voltage (HV) power supply with a switching system. The chamber is evacuated, then the plasma-forming gas, e.g., methane, is backfilled into the chamber. A plasma is ignited, e.g., as a direct current (DC) glow discharge, mostly thermionically assisted, or by radio
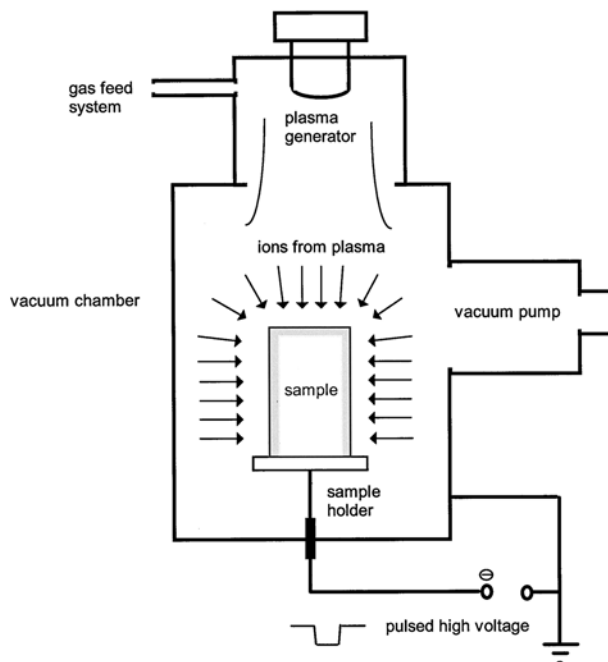
Fig. 1. Simple sketch of setup for PBII.

frequency (RF) or microwave excitation, the latter often in the electron cyclotron resonance (ECR) mode. The sample holder is biased and ions from the plasma are accelerated towards it. They are implanted from all sides at a time; only the electrical contact point is shielded.

Figure 2(a) shows an example of a PBII apparatus. It consists of a cylindrical vacuum chamber with a pumping system at the backside (not visible), and an electron cyclotron resonance (ECR) plasma source on top. The upper part of the chamber is surrounded by a solenoid electromagnet for plasma confinement. Through the opened loading door, the sample holder with a cogwheel on it can be seen (Fig. 2(b)). A view through a sapphire flange during the process shows the sample immersed in the plasma (Fig. 2(c)).
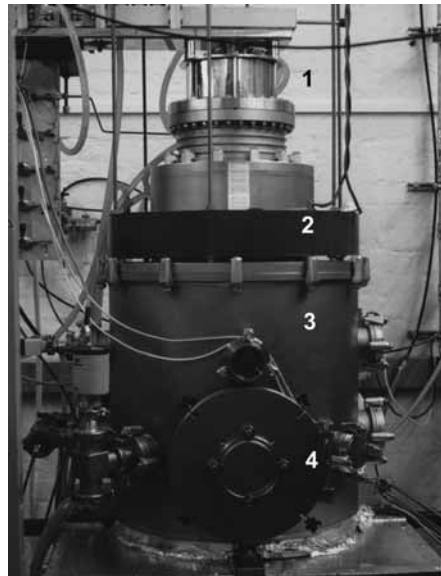
(a)
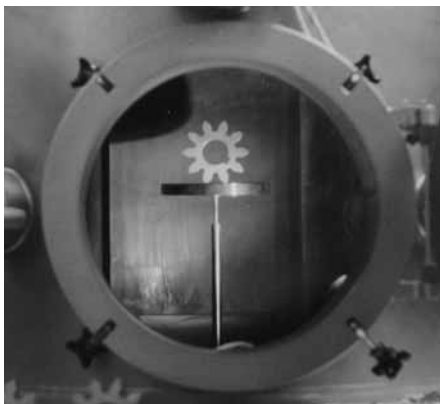
(b)
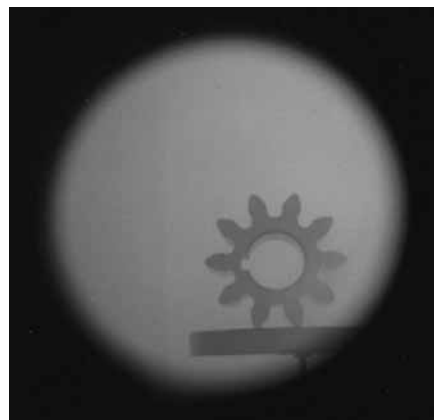
(c)

Fig. 2. (a) PBII apparatus with 1) ECR plasma source on top, 2) solenoid for plasma confinement, 3) vacuum chamber, 4) chamber door; (b) opened chamber with sample holder and sample; (c) view through window during process.

The samples are usually pulse-biased. This has to be done to be able to achieve the high bias voltages which is not possible in a DC or CW (continuous wave) mode. The currents during pulse application can be very high. The power going into the sample has to be controlled by pulse length and pulse repetition rate.

Figure 3 shows schematically what is happening during high-voltage pulse application. The sample is negatively biased, usually as a high-voltage pulse in the range of several kV to tens of kV. Electrons which are moving fast are repelled in the electrical field (Figs. 3(a) and 3(b)). The relatively slow ions are left back and form an ion matrix sheath. Within the sheath, they are accelerated towards the sample and implanted (Figs. 3(b) and 3(c)). The plasma sheath expands. Then, the pulse is switched off (Fig. 3(d)). The plasma around the sample regenerates.

Technical details and applications, historical development, and examples of results both in metallurgical and semiconductor fields of PBII can be found in a monograph and reviews .[1,3,4]

PBII has been developed by Conrad and coworkers, initially for nitrogen ion implantation into nonflat objects to circumvent the geometrical restrictions of conventional beamline ion implantation.[2,6] When nitrogen is used for implantation in order to form nitrogen solid solutions or nitride phases, it is a logical consequence to try hydrocarbon gases such as methane or acetylene for carbide formation. However, between nitrogen and carbon, there is a basic difference: nitrogen is a gas, whereas carbon is a solid. Therefore, PBII as a plasma method will not only lead to carbon implantation but also to carbon deposition, in analogy to plasma-enhanced chemical vapor deposition. PBII is carried out by pulse-biasing the sample. During high-voltage pulse application, ions from the plasma-forming hydrocarbon gas, e.g., CH_4^+, CH_3^+, and also CH_5^+ and $C_2H_5^+$ from gas phase reactions in the case of a CH_4 plasma, are accelerated towards the substrate/target and impinge there with high kinetic energy. These ions, when they have the full kinetic energy given by the pulse voltage, will be implanted into the target. During the time when the pulse is off, deposition of a thin film will take place, in principle PE-CVD. In this case, radicals play an important role,
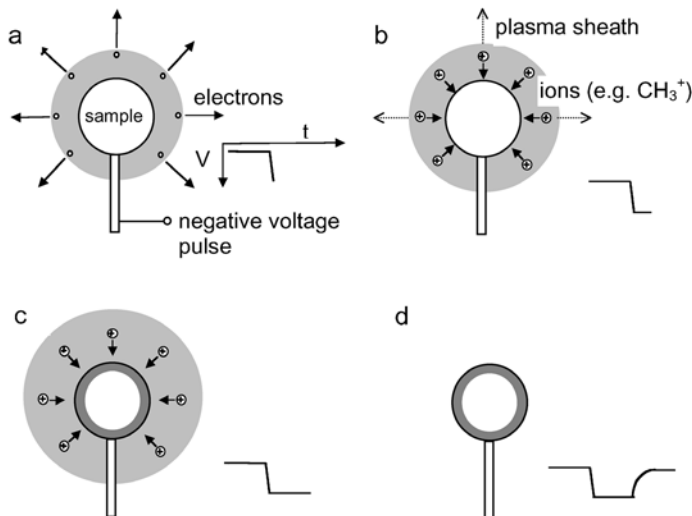
Fig. 3. Processes around sample during high-voltage pulse.

particularly the CH$_3$ radical which is most abundant in a CH$_4$ plasma. In PBII, in contrast to PE-CVD, there is the influence of the high energy ion irradiation during pulse application. Apart from ion implantation and deposition, ion beam mixing based on recoil implantation with forward and backward sputtering of atoms in the growing film or in the interface between film and substrate plays an important role. These effects can be used to form DLC films, different from those formed by other methods such as sputtering or PE-CVD.

Another PBII technique is based on plasmas generated from solids by the arc technique.[7,8] It is also called plasma-based ion implantation and deposition (PBIID), or plasma immersion ion implantation and deposition (PIIIaD). This technique is well described in ref. 1 and is not considered here. The present review is limited to PBII with hydrocarbon plasmas. In the following, the properties of PBII a-C:H or DLC films from hydrocarbon plasmas will be discussed with examples from the literature. Issues such as different PBII techniques, different plasma-forming hydrocarbon gases and gas mixtures, variations in the process parameters such as bias voltage and gas pressure, and their influences on the film properties, such as structure and hydrogen content, and the applications of the resulting films will be addressed. The applications mainly aim at friction and wear reduction; in a few cases also corrosion is looked at. Mostly, the process parameters are provided so that the reader will gain information on their range and influence on the DLC properties.

2.   First Experiments: DLC Films on Steel and Titanium-Alloys for Wear and Corrosion Protection, Formed in Methane Plasma

Historically, DLC formation by PBII began in the USA; then, it was also investigated in other countries. Presently, Japan and China are most active in the field.

The first experiments on hydrocarbon PBII were carried out by Conrad and coworkers in the early 90s, after they had initially developed PBII for nitrogen implantation.[9,10]

The main purpose of their experiments was carbon ion implantation, rather than DLC deposition. Then, it was found that a combination of both, carbon implantation and carbon deposition, is favorable.

Chen *et al*. used hot-filament and glow-discharge plasmas of methane.[9] One sample was grounded to deposit a carbon film without the influence of a bias voltage. Further DLC films were formed with bias voltages of –2, –12, and –30 kV. At the largest voltage, a carbon-implanted region with a 30 nm carbon film on top was formed. Transmission electron microscopy (TEM) showed that all films were amorphous. The friction coefficients were tested against a 3 mm ruby ball by a pin-on-disc tester without lubrication at a relative humidity of 50%. The normal load was 0.49 N; the disk rotated at 54 rpm at a diameter of 5 to 8 mm. Table 1 shows a comparison of the friction coefficients after 1620 cycles of wear. Films deposited without bias showed the highest coefficient, those with low or high bias exhibited similar values, and the best result was obtained for the DLC formed at –12 kV. Profilometric measurements of the wear grooves gave 200 nm for the film deposited without bias, and were not measurable for the PBII films. This shows the beneficial effect of the treatment.

The authors ascribe the differences in the performance of PBII films from those formed without ion bombardment to the effect of the incident energetic ions and their knock-on atoms. They lead to the formation of a carbon network with favorable tribological features, i.e., the DLC.

Table 1
Film thickness and friction coefficient of samples treated by methane PBII; data from ref. (10).

Pulse bias (kV)	0	–2	–12	–20
Film thickness (nm)	200	150	60	30
Friction coefficient	0.35	0.14	0.08	0.15

In further experiments, Chen *et al.* treated AISI 304 stainless steel and Ti-6Al-4V by hydrocarbon PBII.[11] Prior to carbon implantation, the samples were sputter cleaned by 10 keV argon ion bombardment. The implantation/deposition was carried out in a CH_4 plasma at an acceleration voltage of –30 kV at a pulse peak current of 13.8 mA/cm^2. The implantation dose was 3×10^{17} cm^{-2}. Three repetition rates were used: 42, 87, and 126 Hz. The carbon depth profiles were obtained by Auger electron spectrometry (AES). Figure 4 shows the Auger depth profiles of the stainless-steel samples. An essential feature of DLC-PBII can be seen. At the lowest repetition rate, a 30-nm-thick carbon film on top of a carbide transition zone is formed. At higher repetition rates, the implantation process prevails, and no carbon film is formed. The authors assume that the shallow profile at the highest repetition rate may be due to excessive heating which leads to the outdiffusion of carbon or enhanced sputter etching.

Raman spectroscopy showed that the carbon film is DLC. For the substrate, electron diffraction gave the pattern of metastable hexagonal iron carbide Fe_2C in the case of the lowest repetition rate, and an amorphous structure at the highest.

The wear performance was tested on a pin-on-disc tester against a 3 mm ruby ball without lubrication. After the test, the depth of the wear grooves was measured. Table 2 shows a comparison of the results for the steel. At lower loads, the treatment leads to wear reduction in all cases. The DLC film performs better than the carbide films. This is probably due to lower friction and higher elasticity. Only at the highest load, the performance is no longer good; apparently, the counterbody broke through the film.

In order to test the corrosion performance, the steel samples were subjected to electro-chemical polarization measurements in deaerated 0.1 N sulfuric acid. Table 2 shows the comparison of the corrosion potentials and the metal dissolution currents at a potential of 0.2 V. The plasma treatment shifts the corrosion potential to more noble values, particularly in the case of the DLC film. For the currents, the DLC films lead to a reduction by an order of magnitude compared with the untreated sample. The carbide films are located in between the DLC-coated sample and the untreated sample. These results show that the coating is effective in corrosion protection.

These early experiments demonstrated the feasibility of both DLC deposition and carbide formation by PBII, the influence of the PBII process parameters on the film properties and their beneficial effects both on wear and corrosion.

3. Basic Studies on Correlation between PBII Process Parameters and DLC Properties

3.1 *Acetylene and acetylene/argon plasmas*

Munson *et al.* reported in an early paper on large-area DLC PBII. In their setup, treatment of surface areas up to 3 m^2 is possible.[12] They used C_2H_2 with pulsed biases of –0.2 to –4 kV at high repetition rates of up to 14000 Hz. The alternative technique to PBII in their setup
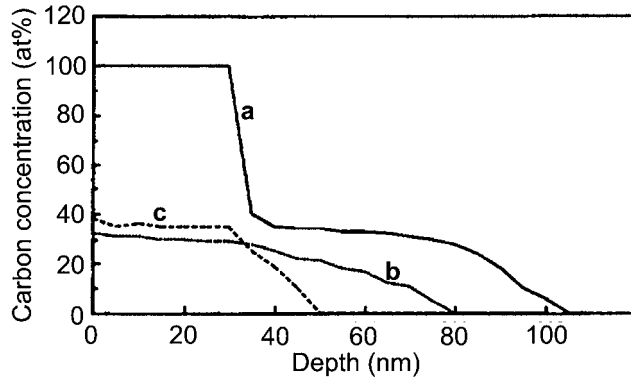
Fig. 4.   Auger electron spectrometric concentration/depth profiles of DLC film on stainless steel, treated in methane plasma at different pulse repetition rates; (a) 42 Hz, (b) 87 Hz, (c) 126 Hz; adapted from ref. 9.

Table 2
Wear depths at different loads, corrosion potentials, and dissolution currents; data were extracted from load vs wear depth plots and from current density vs potential curves in ref. 11.

Sample	Wear depth (μm) at load: 0.2 N	0.49 N	0.98 N	1.96 N	Corrosion potential (V)	Dissolution current at 0.2 V (μA/cm^2)
unimplanted	0.6	0.9	3.5	4.5	–0.9	13
42 Hz	b.l.	b.l.	0.5	4.2	–0.4	1.3
87 Hz	0.1	0.25	1.3	4.4	–0.8	5.8
126 Hz	0.1	0.3	2.0	4.4	–0.8	7.6

b.l.: below limit of detection

was RF deposition driven by the target self-bias. The authors state that in this case, the ratio of the area of the target to that of the grounded process chamber makes it difficult to obtain a desired negative bias voltage. This problem is circumvented when pulse biasing, i.e., PBII, is used.

The hardness of the DLC films for different bias voltages was measured as a function of the C_2H_2 pressure; see Fig. 5. A general trend is that an increase in pressure decreases the hardness. This is probably due to the reduced energy of the ions brought about by gas molecule collisions. This effect can be counterbalanced to a certain extent by increasing the voltage. A voltage of –0.6 kV at a pressure of around 0.27 Pa gives similar results as a voltage of –4 kV at 2 Pa.

Although it is not stated in the paper, higher pressures usually lead to higher deposition rates. If so, one of the advantages of pulse biasing with higher voltages at higher pressures is that hard films can be deposited at larger deposition rates. The authors analyzed the DLC sp^3 content and found a correlation with hardness. Higher sp^3 content leads to higher hardness. One can conclude that higher voltages lead to larger energy and momentum input into the film which, as a consequence, leads to more diamond-like bonding and higher hardness.
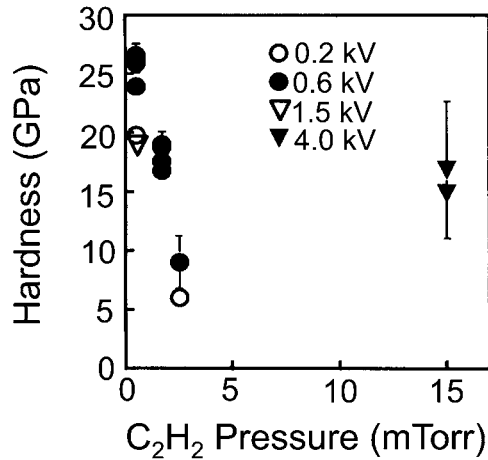
Fig. 5.   DLC hardness as function of acetylene pressure for different pulse bias voltages; adapted from ref. 12.

Lee *et al*. deposited DLC films onto silicon at low pressures (0.04 Pa to 0.93 Pa), bias voltages and pulse repetition rate in a mixed acetylene/argon plasma.[13] They generated an RF plasma of argon and sputter cleaned the substrate at –0.6 kV bias. Then, they introduced C_2H_2 into the argon plasma, and deposited DLC at voltages varied from –0.07 to –0.3 kV at 10 Hz with a pulse length of 20 μs. Thus, they achieved a deposition rate of 1.4 nm/min at a pressure of 0.04 Pa and a 2:1 Ar/C_2H_2 ratio. Rutherford backscattering spectrometry (RBS) gave an argon content of 3 to 4 at%; elastic recoil detection analysis (ERD) showed that the hydrogen content ranged from 25 at% to 30 at%. The film thickness ranged between 100 and 230 nm.

Stress and hardness measurements showed that stress increased with gas pressure, while hardness decreased. Figure 6 shows the dependences of hardness and stress on the bias voltage. For the lowest gas pressure, a maximum compressive stress of 9 GPa was reached, when the voltage was –0.15 kV. In the case of higher gas pressures, the dependence was only weak, and the values remained below 5 GPa. Lower pressure yielded higher hardness values. They ranged between 25 and 30 GPa. Lower pressure also led to better adhering films; and the sp^3 content was higher than for higher pressures, as UV-Raman spectra showed.

The authors explain that the use of argon is favorable for creating an inductive plasma for the hydrocarbons, minimizes the deposition of a conductive carbon film on the plasma source, which hinders inductive plasma generation, and leads to ion beam mixing effects and energy transfer to the growing film of surface neutral carbon atoms.

3.2   *Comparison of methane, acetylene and toluene plasmas*

Volz *et al*. used an ECR methane plasma to bombard Si(100) with hydrocarbon ions.[14] The pulse duration was 15 μs, the repetition rate was 600 Hz, and the bias voltage was –45 kV. RBS showed that this process led to carbon implantation into silicon, followed by the build-up of a DLC film when the process time or pulse number was increased. At a pulse number of 2.1×10^6, a DLC film was formed on top of an amorphous Si-C gradient film.

By RBS and nuclear reaction analysis with the $^1H(^{15}N, \alpha\gamma)^{12}C$ reaction for hydrogen analysis, a complete element depth profile could be obtained.[15] Figure 7 shows a 50-nm-thick DLC film with around 17 at% hydrogen incorporated, followed by a 150-nm-thick
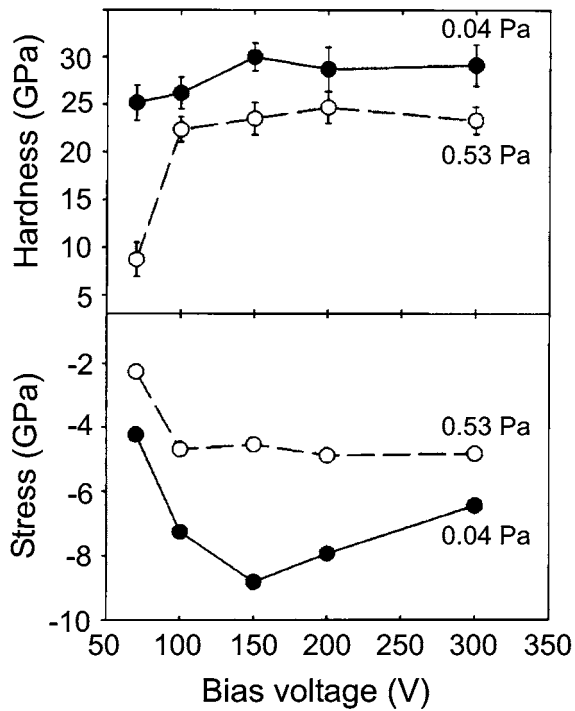
Fig. 6.   Hardness and stress of DLC films as functions of bias voltage for two different pressures; adapted from ref. 13.
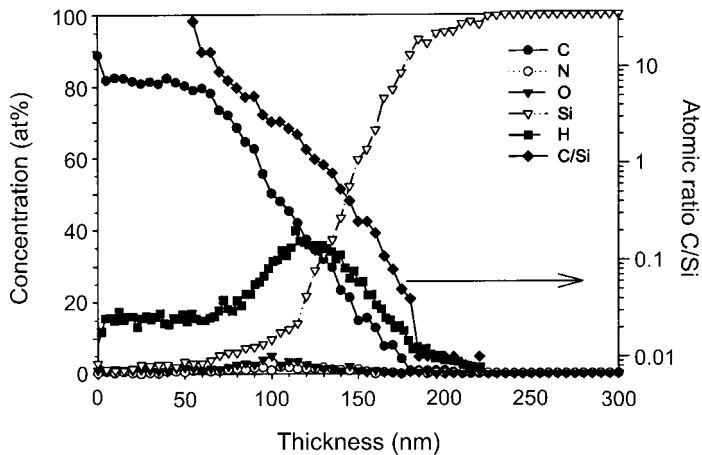
Fig. 7.   Concentration vs depth profile of all elements and atomic C/Si ratio of Si wafer, bombarded with 2.1×10^6 pulses at –45 kV; adapted from ref. 15.

gradient Si-C-film with a maximum hydrogen concentration of 35 at%. The hydrogen is implanted only slightly deeper than the carbon. However, this is not an implantation profile, but the hydrogen more or less follows the carbon. Hence, this is a chemically governed effect.

Volz *et al*. compared methane and toluene as plasma-forming gases.[16] Under the same process conditions, in the case of methane 5.4×10^5 pulses give no DLC film, but a Si-C layer; however, for toluene, 120 nm DLC were deposited. This is explained by two effects: in the case of toluene, C-C bonds are already preformed. Different hydrocarbon molecules are deposited on the surface and grow a DLC film. Another effect is, that in the case of toluene the average energy per atom of impinging molecules is much smaller than for methane. This means that methane will form a thicker Si-C implantation zone, while toluene will form a thin transition zone, but a thick DLC deposit. The film formed with toluene was examined by X-ray photoelectron spectrometry (XPS). Figure 8 shows the development of the XPS C1s signal with sputter etching time, i.e., at different depths in the sample. At the surface, a C-C bond is found. Upon sputtering, with increasing depth the chemical shift is moved to lower binding energies, indicating a Si-C bond, then the signal vanishes. This shows that the film is composed of a thick DLC film on top of a Si-C transition layer. The film has been characterized by Raman spectroscopy. An 80-nm-thick film showed an intense broad Raman signal with the typical D- and G-bands of DLC, indicating a large fraction of sp^3 bonding.

Miyagawa *et al*. used pulsed RF plasmas of methane and toluene to form DLC films.[17] The substrates were silicon wafers. They were sputter-cleaned with argon ion bombardment; then carbon was implanted with a methane plasma at –20 kV to form an implantation transition layer, and the DLC films were formed with toluene at –5 to –20 kV. The pulse width was 5 µs; the repetition rate was 200 Hz. The processing times were 5 min for methane treatment and 60 min for DLC deposition. XPS measurements gave a C1s peak composed of C-C (sp^3), C=C (sp^2) and some C=O. The sp^3/sp^2 ratio was 0.28. Table 3 shows a comparison of hydrogen content, as obtained by ERD, and thickness for the different bias
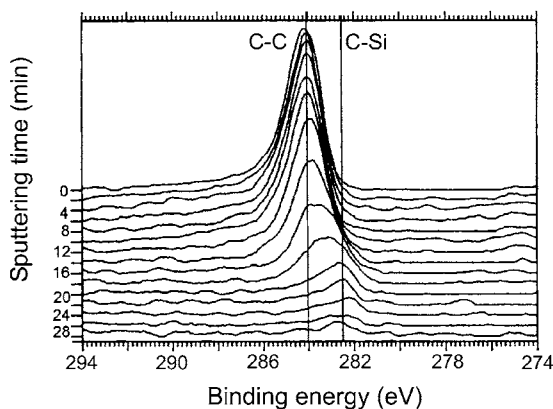
Fig. 8.   Series of C 1s XPS spectra at different sputtering times of sample treated in toluene plasma; adapted from ref. 16.

Table 3
Hydrogen content and thickness of DLC films, obtained at different bias voltages; data from ref. 17.

Bias voltage (kV)	–5	–10	–20
Hydrogen content (at%)	15.5	15.0	22
Thickness (nm)	250	220	150

voltages. The films showed a hydrogen content between 15 and 22 at%. The deposition rate decreased with increasing voltage. This is due to an increase in sputter etching.

This is an example of the formation of a carbide transition layer from the substrate to the DLC film.

Baba and Hatada carried out a number of studies on the deposition of DLC films.[18] They used both CH_4 and C_2H_2. The pulse voltage was varied between 0 and –18 kV; the repetition rate was 100 Hz, and the pulse length was 100 μs. In some cases, additionally the sample was biased with a DC voltage of several kV. Figure 9 shows Auger depth profiles. While methane led to carbon ion implantation, with a gradient film of carbon in silicon, the use of acetylene gave a DLC film. Raman spectroscopy showed that without the use of high-voltage pulses, the ratio of I_D/I_G bands remained below 1, while under PBII conditions it was around 1.5. A reduction in this ratio indicates that PBII reduces the graphitelike character of the films.

Liao *et al.* investigated the features of DLC films deposited on Si (100).[19] They bombarded the wafer with argon ions at –2 kV to remove contaminations. For DLC deposition, acetylene was used. The bias voltage was –18 kV, the pulse width was 45 μs, and the repetition rate was 80 Hz. With a deposition rate of 1 nm/min, process times of 5 to 60 min led to nanometer films of corresponding thickness. Figure 10 shows the XPS depth profiles of 10-nm- and 30-nm-thick films. A broad transition between silicon substrate and carbon film can be identified. Raman spectroscopy showed the typical broad band with D- and G-band at 1544 and 1366 cm^{-1}, respectively. From the I_D/I_G ratio, the authors conclude that the films show a high sp^3 content. The chemical shifts in XPS show both C-C bonds and Si-C bonds in the transition region between carbon film and silicon substrate. The SiC phase reduces the interface energy and thus enhances adhesion.

IR spectroscopy gives information about the C-H bonds. The spectra show bands which can be assigned to sp^3 CH, CH_2, and CH_3 bonds, to a lesser extent to sp^2 bonds. This is in agreement with the Raman results. The authors explain that sp^3 bonds are formed when high ion energies and rapid quenching rates are present, which is the case in PBII. Atomic force microscopy (AFM) results show that the films are very smooth. For the 30-nm-thick film, a roughness of 0.25 nm is found.

Tojo *et al.* formed DLC films on silicon or tungsten carbide (WC) substrates.[20] In their setup, both radio frequency and negative high-voltage pulses are applied to the samples through a single feedthrough. They used both methane and acetylene. The pulse bias voltage was varied from –3.5 to –10 kV for DLC deposition. Prior to that, carbon was implanted at –20 kV in order to form a transition layer. Hardness measurements showed that both hardness and deposition rate were higher for the acetylene plasma than for the methane plasma. Methane gave a hardness value of 11 GPa, whereas it was 15 GPa for acetylene. At the higher process pressure of 2 Pa, the films showed relatively low compressive stress (0.35 GPa). The stress decreased with increasing pressure, as can be seen in Fig. 11.

In an attempt to form SiC films, Ueda *et al.* treated (001) silicon wafers in a methane ECR plasma at a comparatively high pulse repetition rate of 1250 Hz with 5 μs pulses at a –35 kV bias voltage.[21] Auger electron spectrometric depth profiling gave an unexpected result. The sample which had been treated for only 2 min gave a 20-nm-thick DLC film and a carbon gradient with a thickness of 50 nm (see Fig. 12), while those treated for 10, 20 or 100 min gave no carbon film, but a carbon implantation profile. For the longest treatment time, the
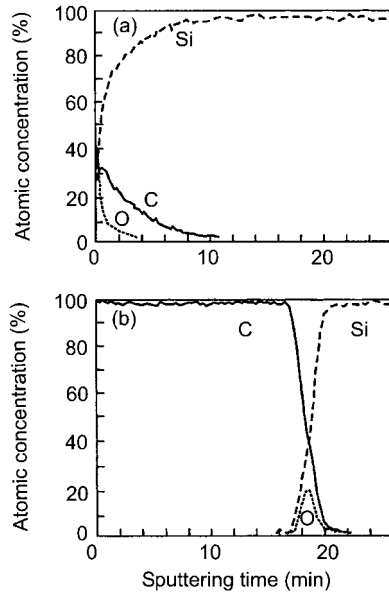
Fig. 9.   Auger concentration/depth profiles of silicon wafers treated by (a) CH_4, -18 kV (b) C_2H_2, -15 kV/-3kV DC; adapted from ref. 18.
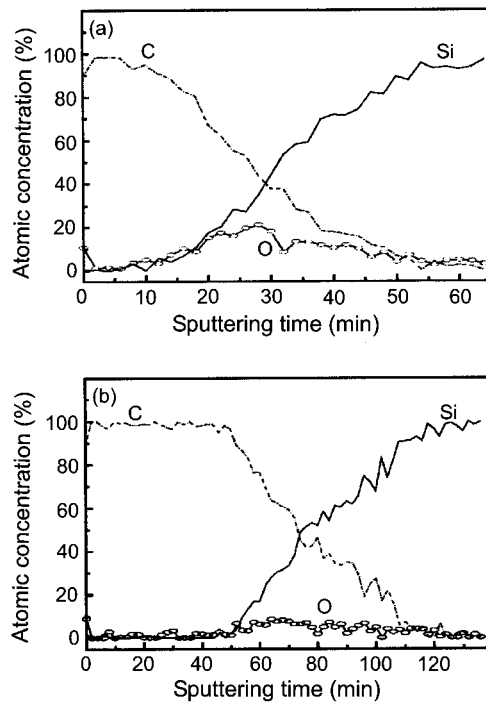
Fig. 10.   XPS element concentration profiles of (a) 10-nm-thick film, (b) 30-nm-thick film; adapted from ref. 19.
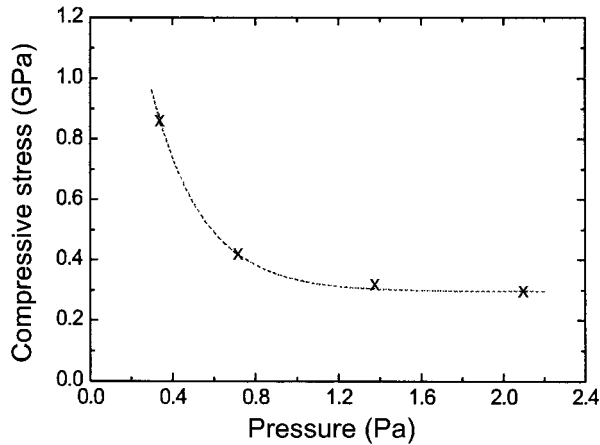
Fig. 11.   Compressive stress of DLC films as function of C_2H_2 process pressure; the bias voltage was –5 kV; adapted from ref. 20.
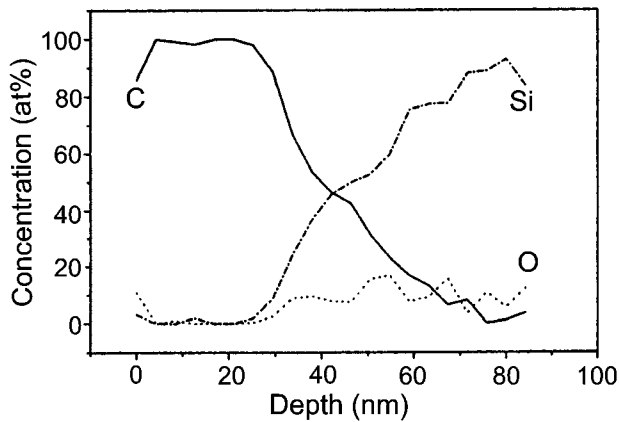
Fig. 12.   Auger concentration vs depth profile of silicon wafer, treated in methane plasma at –35 kV; adapted from ref. 21.

film reached 80% carbon in its maximum at a thickness of 100 nm. The authors assume that the carbon layer was removed by sputtering at the longer process times. The temperature may also play a role, as it reached 450°C for the 100 min treatment, but stayed below 200°C for the 2 min process.

Similar to that of DLC films, the formation of SiC also depends on the PBII mode used. An *et al.* generated the plasma by self-ignited glow discharge when the voltage pulse was applied to the sample.[22] They used methane at –15 kV and acetylene at –25 kV with large pulse widths of 550 and 300 µs, and received in both cases no DLC deposition, but carbon implantation. This is because no external plasma source was used. During the pulse-on time, implantation mainly occurred; during the pulse-off time, the plasma was quenched and no film was deposited.

3.3   *DLC deposition onto three-dimensional objects: cylinders and tubes, wedges and trenches*

It is a special feature of PBII that three-dimensional objects can be treated. A challenge among these are cylinders and tubes.

The first experiments on coating cylinders, both outer and inner walls, were carried out by Malik *et al.*[23] They used methane or acetylene as plasma-forming gases. For cylinder-coating of the inner walls, a coaxial configuration in a cylindrical vacuum chamber was used. A central electrode was placed inside the cylinder. It was kept either at RF bias or at ground potential. When it was biased, a radial electrical field normal to the inner cylinder wall was generated. The high-voltage ignited a glow discharge. In order to enhance the plasma, the electrode was used as an RF antenna. The outer walls of cylinders were coated using an aluminum tube around the cylinder as a housing. The voltage pulses were generated between the substrate and the aluminum housing. Two cylinder types were used; for the outer coating, one with a length of 12.7 cm and 6.35 cm diameter; for the inner coating, one with a length of 50 cm and an inner diameter of 10 cm.

In the case of DLC deposition on the outer wall, experiments were first carried out without the housing. This led to a nonuniform coating. For the experiment with the housing, the substrate was first bombarded with argon ions for sputter cleaning, then methane was used for carbon implantation, eventually acetylene was fed into the chamber and a DLC film was deposited at –5 kV, 100 μs pulse width, and 100 Hz. This procedure led to DLC films with good adhesion. Figure 13 shows that there is a certain distribution in thickness. Although it is around 1 μm in the center, it is 0.8 μm close to the ends of the cylinder. The authors explain this difference as being caused by a more uniform distribution of the plasma inside the cylinder. The plasma is generated as a glow discharge due to the bias of the cylinder; the coaxial electrode is grounded on both sides. The carbon ions at the center might have more residual time than those at the ends.

The authors state that the thickness distribution is reasonably uniform for tribological application.

Baba and Hatada developed a PBII method for treating the inner walls of tubes.[24] The plasma was generated by a coaxial ECR discharge. A magnetic field of one kilogauss was generated by a solenoidal coil around the tube. It could be moved along the tube to get uniform treatment along the tube axis. They deposited DLC films from acetylene plasma on AISI 304 and 316L stainless-steel tubes with different dimensions. One was a large tube with a 1 m length and a 35 mm inner diameter, another one was 5 mm long with a 0.9 mm inner diameter, and also bundles of small tubes were coated. The large tube was treated at –15 to –20 kV, 100 Hz and 50 μs pulse length. Figure 14 shows the film thickness at four different locations in the tube, obtained from cross-sectional scanning electron microscope (SEM) observation. The entire tube was coated with a very good uniformity.

The authors tested the corrosion protection effect by potentiodynamic polarization experiments in 5% sulfuric acid.[26] The potential scan rate was 1 mVs^{-1}, the scan range was from –0.5 V to +1.7 V vs Ag/AgCl electrode. They compared the DLC film with films produced by nitrogen and oxygen PBII. Table 4 shows the metal dissolution at different potentials. The DLC coating performed considerably better than the oxygen and nitrogen implants.
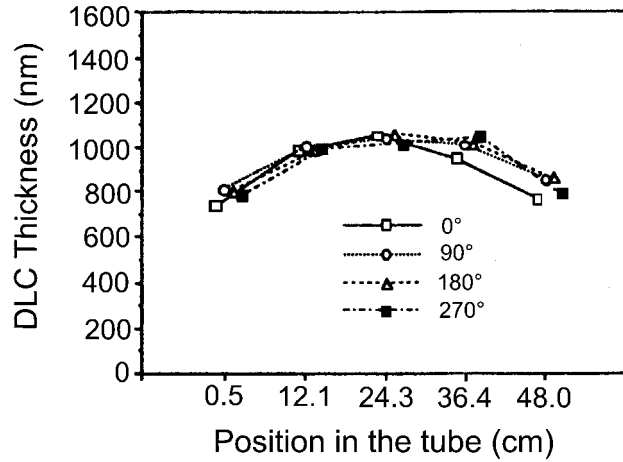
Fig. 13.   Thickness distribution of DLC films on inner surface of cylinder at different circumferential positions; adapted from ref. 23.

(a)
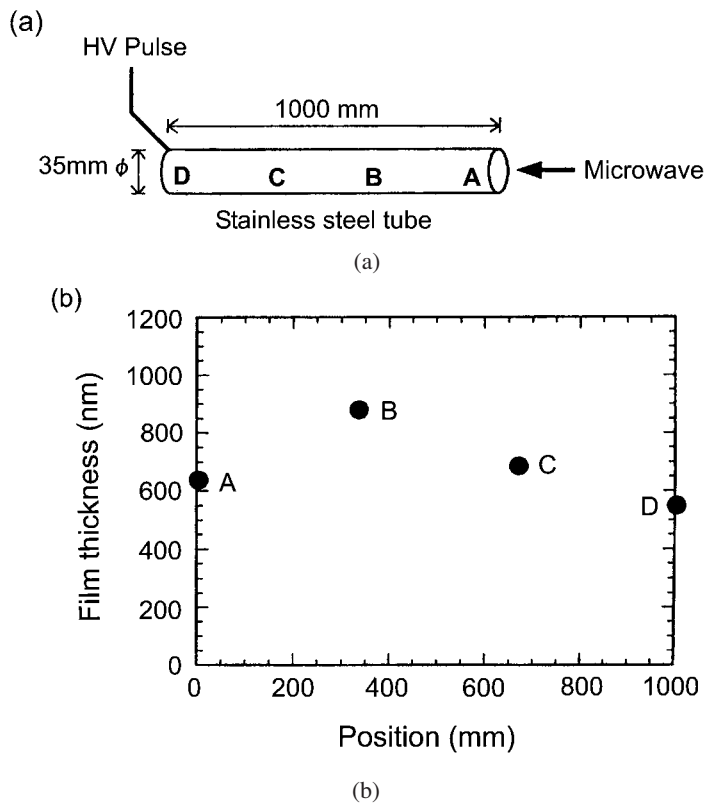
Fig. 14.   (a) Deposition onto inner wall of tube of 1 m length, (b) film thickness distribution on inner tube wall; adapted from ref. 25.

Table 4
Anodic dissolution currents at different potentials of differently treated 316L stainless-steel tubes; data were extracted from ref. (27).

Treatment	Untreated	Oxygen PBII	Nitrogen PBII	DLC PBII
Anodic current at –0.5 V (A m^{-2})	6×10^{-2}	2×0^{-2}	0.3×10^{-2}	3×10^{-2}
Anodic current at –1.5 V (A m^{-2})	2×10^{2}	2×10^{2}	2×10^{2}	8×10^{-3}

Small tubes with a length of 15 mm and an inner diameter of 0.9 or 0.5 mm were arranged in a bundle, and treated at a pulse voltage of –10 kV, a repetition rate of 1000 Hz and a pulse duration of 10 μs.[27] The tubes were analyzed using a light microscope and Raman spectroscopy. The results showed that the tubes could be coated, despite their small diameter. For the used setup, the homogeneity of the DLC films and their structure depend on the acetylene flow rate, the inner diameter of the tube and the number of tubes in the bundle.

Nishimura *et al*. used a PBII technique in which the substrate itself was used as a RF antenna for plasma production.[28] The plasma-forming gases were CH_4, C_2H_2, and $C_6H_5CH_3$ (toluene). The process consisted of four steps: sputter-cleaning of the substrate with a 50:50 gas mixture of Ar and CH_4 at –10 kV, followed by carbon ion implantation at –20 kV with a repetition rate of 1000 Hz with a pure CH_4 plasma, then change of gas to C_2H_2 to form a graded mixing layer under the same conditions, and eventually a rapid deposition with a rate of around 1 μm/h of DLC using $C_6H_5CH_3$. The DLC film thicknesses were 2 to 4 μm. The substrates were made of aluminum-alloy A5052: a tube with a diameter of 25 mm and a length of 150 mm, three triangular prisms with different wedge angles and a length of 90 mm, and three trenches with different aspect ratios.

By combining toluene gas and ion implantation, the residual compressive stress of DLC film remained at low values from 0.2 to 0.35 GPa. The hardness measured using a nanoindentor was 12 GPa. For the pipes and triangular prisms, the thickness profiles were almost uniform on the whole surfaces. Figure15 shows the film thickness profile of a trench with both width and depth of 10 mm (aspect ratio of 1). The film thickness at the top surface was about 1.3 times larger than that of the bottom and 1.9 times that of the sidewall. In the scratch adhesion test, no flaking, indicating adhesive failure, was observed.

This example shows that by a combination of implantation and deposition using different gases, gradient films with very good properties can be deposited onto three-dimensional objects.

Watanabe *et al*. used an ECR plasma source with a mirror field for depositing DLC films.[29,30] The substrates were silicon (100) wafers, placed on the surface of a concave or convex substrate holder. Methane served as plasma-forming gas. For convex faces, film thickness was almost uniform, independent of the deposition conditions. This is due to a uniform plasma surrounding the substrate. For concave faces, the thickness of the films decreased when the microwave-incident angle was decreased. This was found for samples which were deposited with pulse bias. When an additional DC bias was used, the uniformity became considerably better. The authors ascribe this to a continuous supply of ions in the plasma to the samples. In tribological tests, the samples gave a friction coefficient of 0.02. No flaking was observed even at a load of 20 N.
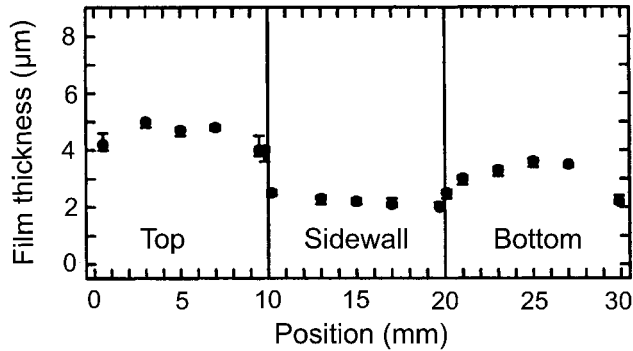
Fig. 15.   Film thickness profile on trench with aspect ratio of 1; adapted from ref. 28.

4.   Application-Oriented Studies: Reduction of Wear and Corrosion of Metals

4.1   *Aluminum alloys*

Nastasi *et al*. used comparatively low bias voltages at a high repetition rate to form DLC coatings on silicon and on A390 alloy, a highly eutectic aluminum alloy with 18% silicon which is used in the automotive industry.[31] The bias voltages ranged from –0.2 to –0.6 kV, the pulse width was 20 μs, and the repetition rate was 12×10^3 Hz. The gas was acetylene. At high pressure (0.33 Pa), the plasma was formed by the pulse voltage; at low pressure (0.07 Pa), an independent antenna was used to generate the plasma. In some cases, carbon implantation was performed prior to DLC deposition. In this case, an RF-coupled plasma at low pressure (0.04 to 0.09 Pa) was employed. Pulses of 20 μs at –20 kV at 400 to 600 Hz were used.

Measurements of hardness and elastic modulus for each of two different gas pressures and bias voltages show the following trends: both hardness and elastic modulus decrease with increasing pressure, and increase with bias voltage; see Table 5.

Friction and wear were examined with a pin-on-disk tester under dry sliding conditions. 52100 steel pins and ruby pins were used at loads of 0.8 and 4.5 N. Figure 16 shows the average friction coefficient for different loads and pins as a function of relative humidity. In general, the friction coefficient of the ruby pin is lower than that of the steel pin. In the case of the ruby pin, it is not dependent on load. However, it shows an increase with humidity. For the steel pin, humidity plays a minor role, but the coefficient increases with load. Hardness measurements and hydrogen analysis showed that the hardness decreases with hydrogen content. The wear rate shows the same trend; see Table 6. An increase in hardness from 9 to 24 GPa led to a reduction in wear by a factor of 3.

In other words, a lower gas pressure led to less hydrogen incorporation and yielded films with higher hardness which were more wear resistant.

For coating aluminum alloy A390, a four-step process was developed. Figure 17 shows a schematic presentation. First, the alloy was sputter-etched with Ar ions at voltages from

Table 5
Hardness and elastic modulus of DLC films formed at different acetylene gas pressures and bias voltages; data were extracted from ref. 31.

Gas pressure (Pa)	Hardness (GPa) at voltage 0.2 kV	Hardness at 0.6 kV	Elastic modulus (GPa) at 0.2 kV	Elastic modulus at 0.6 kV
0.07	20	24	165	205
0.33	6	9	50	80
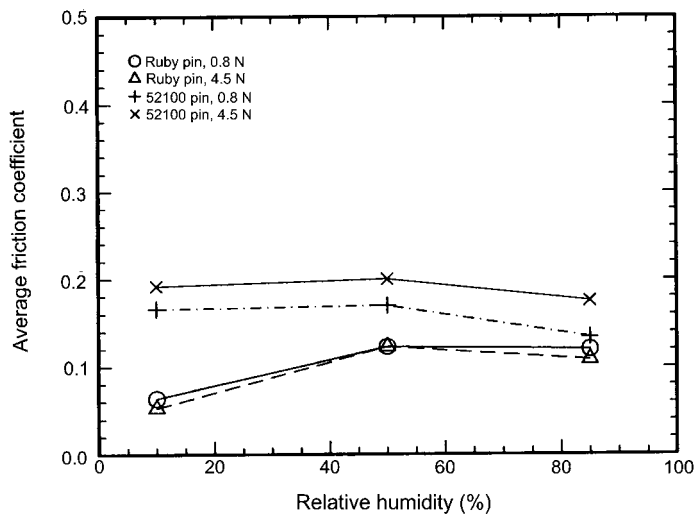
Fig. 16. Friction coefficient as function of relative humidity for steel and ruby pins at low and high applied loads; adapted from ref. 31.

Table 6
Hardness, hydrogen content and wear rate of DLC films formed at bias voltage of –0.6 kV; data were extracted from ref. 31.

Hydrogen content (at%)	Hardness (GPa)	Wear rate (10^{-6} mm^3 /Nm)
27	9	0.045
22	24	0.014

–1 to –1.4 kV in order to clean the surface and remove contaminations and oxides. Next, carbon was implanted from a methane plasma at a bias voltage of –20 kV to form a carbon graded interface. After it had turned out that the carbon film deposited during the implantation step was not of good quality, as it is mostly graphitic, a second sputter etching step with argon ions was used. The surface layer was removed and the implanted carbon came to the surface. In this way, an excellent transition layer was formed for the final step, namely, DLC deposition at –0.6 kV from acetylene. The DLC coating was 4 to 5 μm thick.

Adhesion tests showed that this procedure led to much enhanced adhesion compared with directly deposited DLC films. Data from pin-pull tests of 16 different DLC deposition runs, which took place within five weeks, gave pull strength values from 30 to 55 MPa. The friction coefficients from pin-on-disc measurements with a 0.15 N load after 12000 cycles
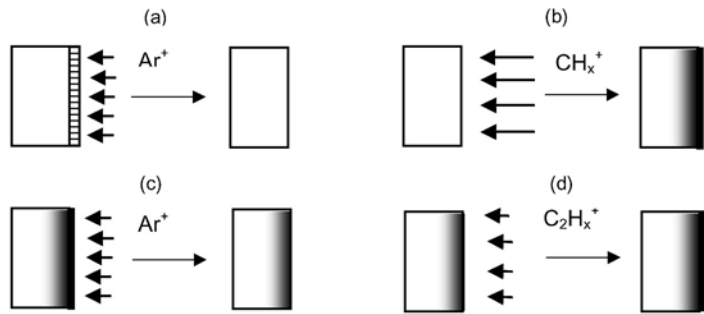
Fig. 17.   Schematic presentation of PBII process for deposition of well-adhering DLC films; (a) Sputter etching of substrate, (b) carbon ion implantation and deposition, (c) sputter etching of graphitic carbon film, (d) deposition of DLC; the precursors of the ionic species are argon, methane, and acetylene; after ref. 31.

were around 0.2. The authors conclude that this technique allows one to reproducibly fabricate DLC films with desirable tribological coatings, e.g., for improving engine components.

Malaczynski *et al*. carried out several tribological tests to evaluate the performance of DLC coatings on aluminum alloys used for fabricating pistons.[32] Pin-on-disk tests under unlubricated conditions with a DLC-coated A390 steel pin running against bare A390 disks and against DLC-coated disks with Hertzian pressures of 1800, 2200 and 2500 psi showed that the friction coefficient in all cases remained below 0.6 while the predefined threshold value was 0.8. This was true for a test duration of 11000 cycles, which was much longer than the required 1500 cycles. For automotive components, thermal stability is required. The samples were thermally cycled from 200°C up to 400°C. For all temperatures, the samples exhibited a friction coefficient of 0.4 for the whole duration of 11000 cycles. Another test was performed using the Cameron-Plint reciprocal tribometer. The friction coefficient of the section of a piston is measured as a function of time to failure, when the coefficient rises. In this case, a load of 70 N with a stroke of 8.6 mm at 6 Hz frequency was used. Figure 18 shows how the time to failure depends on the thickness of the DLC coating. The results show that the performance improves with film thickness. The authors interpret this result as a measure of the time until the coating is worn through. The variations of time to failure for films of the same thickness are due to different contact areas between a piston and a counterbody when they are misaligned.

In an engine dynamometer test, A390 pistons coated with 1.5 μm DLC were run against custom-made bare A390 bores for several hours. After the test, the engine block was disassembled and every part was inspected. No sign of wear could be found. The DLC coating remained intact.

Later, Malaczynski *et al*. published further results on the films formed by the multistep procedure.[33] Initially, the carbon implantation dose was in the range of $2–3\times10^{17}$ cm^{-2}. However, it was then noticed that a higher dose in the range of 10^{18} cm^{-2} which approaches saturation gives better adhesion results. Therefore, pulse repetition rate was increased from 1000 to 5000 Hz, pulse width was increased from 10 to 50 μs, and bias voltage was reduced from –20 to –12 kV. With these parameters, in a 1 h process time, a saturation dose for the formation of aluminum- and silicon-carbides was achieved. Larger process times led to the formation of nonbonded carbon. As mentioned before, carbon was deposited at the surface. For improved adhesion between the substrate and the DLC film, this carbon was detrimental.
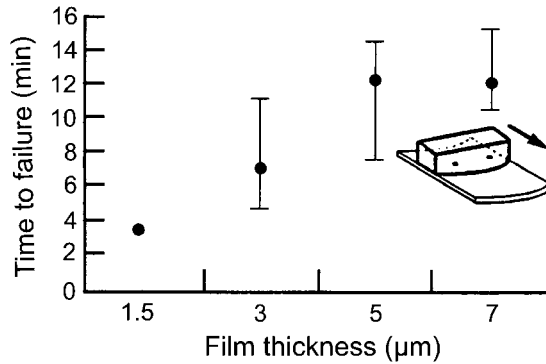
Fig. 18. Time to failure of DLC coating on A390 piston as function of thickness; adapted from ref. 32.

It had to be removed in order to establish a direct contact between the substrate carbides and the DLC film. The film was sputtered away until a stoichiometry of Al_4C_3 was used, which is the stable aluminium carbide phase. For this purpose, as much as 250 nm had to be removed, as experiments with XPS showed. The etch was performed with –2 kV argon ions at 5000 Hz. Eventually, the DLC film was formed in process times of 6 to 8 h with pulse voltages of –4 to –6 kV at 5000 Hz. The gas pressure was in the region of several Pa. In this pressure regime, ions and neutral molecules collide and the kinetic impact energy of the ionic species is lower than the acceleration voltage. High pressure and plasma density led to a faster deposition rate. The typical values were 0.6 to 0.8 μm/h.

Pin-pull adhesion tests with epoxy glue were performed not only for the A380 alloy but also for titanium, which is interesting for areospace and biomedical applications, and chromium and tungsten carbide, which are used in the tool industry. In these cases, again the graded carbide layers act as a transition layer between substrate and coating, thus enhancing adhesion.

Li *et al*. coated LY12 aluminum alloy with DLC films.[34] Prior to coating, the samples were cleaned by 1 kV argon etching. An acetylene plasma, sustained by a hot-filament discharge, was used for deposition. Samples were treated for 2 h using –20 kV pulses with a pulse length of 27 μs and a repetition rate of 128 Hz. XPS spectra showed an asymmetrical peak with a shift of 0.225 eV from the typical graphite C1s binding energy of 284.15 eV towards 285.5 eV, the diamond C1s binding energy. This indicates that the DLC films have a certain sp^3 bonding character. Surface morphology was investigated by atomic force microscopy (AFM). The authors assume that the wettability of aluminum by carbon atoms is low. As the number of carbon atoms to ions impinging per unit time is not very high, the formation of critical carbon nucleation centers for film growth is difficult. However, nucleation centers are formed by incident ions because of their high kinetic energy. They form random nucleation sites, with film growth taking place at many sites at a time. This governs the topography.

4.2   *Steel*

Zeng *et al*. combined DLC PBII with metal PBII with a vacuum arc.[35] They treated 9Cr18 martensitic stainless steel (AISI 440) that is used as a bearing material in aerospace industry. The authors state that the bearings suffered from tribological failure and therefore

they aimed to improve the performance by PBII treatment. They preimplanted tungsten or titanium at –25 kV for 0.5, 1 or 2 h, then they deposited DLC by PBII with acetylene at –30 kV at 30 μs pulse width, and at a repetition rate of 100 Hz for 2 h. AES showed that this led to a 200-nm-thick DLC film on top of a 250-nm-thick metal-containing transition region, with carbon, titanium and substrate atoms mixed, from the carbon film to the substrate. Raman spectroscopy proved that amorphous carbon had been formed.

Microhardness measurements showed that an increase in metal PBII process time led to an increase in hardness; see Table 7. At a load of 0.098 N, the untreated steel showed a hardness of HV690, while the sample treated with tungsten for 3 h gave a value of HV1170. Friction tests gave a value of around 0.8 for the untreated substrate, and around 0.2 for the coated one. The wear behavior was tested versus a 6 mm Si_3N_4 ball at 0.49 N and a sliding speed of 1.5×10^{-3} m/s. An increase in titanium PBII process time from 1 h to 3 h reduced the wear track width by almost half. It turned out that the thickness of the underlying implant zone influences the wear behavior. The more metal is implanted, the lower is the wear. The authors explain this by the thickness of the intermixed transition zone between the DLC film and the substrate.

Shinno *et al.* coated glass substrates and ferrules of a tube fitting (304 stainless steel) in self-ignited plasma PBII in acetylene gas and gas mixtures of acetylene, argon, and oxygen.[36] The pulse repetition rate was 1000 Hz, the pulse length was 10 μs, and the process time was 1 h. Figure 19 shows the dependences of deposition rate on acetylene gas pressure

Table 7
Microhardness and wear test results of stainless steel treated with Ti PBII and DLC PBII; data from ref. 35.

Metal PBII time (h)	Untreated	1	2	3
Microhardness (HV)	690	1020	1090	1170
Wear track width (μm)	220	60	45	36
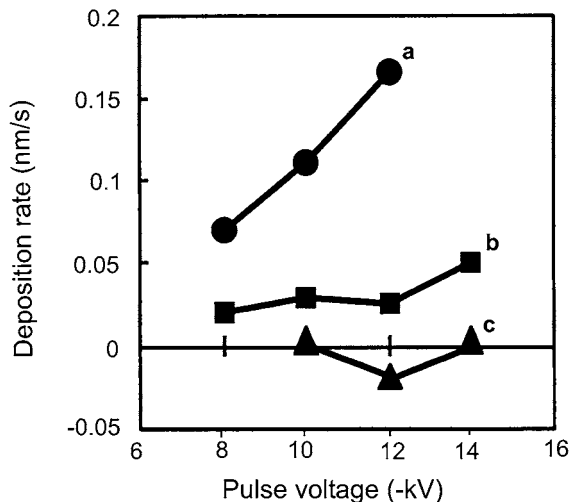
Fig. 19. Dependence of deposition rate on pulse voltage at different gas pressures; (a) 5.3 Pa, (b) 2.7 Pa, (c) 1.3 Pa; adapted from ref. 36.

and pulse voltage. In the high pressure region, at 5.3 Pa, the deposition rate increases with pulse voltage. The density of plasma ions created by glow discharge increases with pulse voltage; as a consequence, more ions are deposited. At lower pressure, this effect is less pronounced, and at the lowest pressure, no more increase can be observed. The efficient deposition rate is around zero or even etching takes place. At lower pressure, the ions have a higher kinetic energy. Thus, sputtering is increased. When oxygen was added to the plasma, the deposition rate decreased with increasing oxygen content and became zero when the oxygen content was about 12% in the gas mixture. This is due to the oxidation of carbon films to volatile oxides.

The deposition of 2.5-μm-thick DLC films on the stainless-steel ferrules led to a loss of adhesion. The films flaked off. These films had been deposited at a constant gas pressure of 5.3 Pa. Apparently, adhesion was not good enough. In order to increase it, the process was modified: rather than using a constant pressure, the pressure was slowly increased and the voltage was decreased, starting from 1.3 Pa at –15 kV, up to 5.3 Pa at –12 kV. Thus, a gradient transition film was formed. At low pressure and high voltage, carbon was implanted; at high pressure and low voltage, a DLC film was deposited. These films showed a good adherence. Thus, 2.5-μm-thick films could be fabricated.

In tube fitting torque mesurements with films of different thicknesses, it turned out that the torque decreased with increasing film thickness. At a rotation angle of 360°, the torques of 0.5-μm-thick films were around 53 to 56 Nm, while those of the 2.5-μm-thick films were below 50 Nm, in one case almost as low as 40 Nm.

Matthews *et al*. used C_2H_2 at a pulse bias voltage of –10 kV with pulse repetition rates ranging from 100 to 800 Hz to deposit DLC onto stainless steel (Staballoy AG17).[27] This material is used for austenitic stainless steel threaded joints for offshore drilling collars. They carried out pin-on-disc tests with a truncated stainless steel cone as the sliding counterface. Table 8 shows a comparison of the critical loads for galling. When compared to TiN and CrN coatings, clearly, the PBII DLC film shows the best results.

The authors carried out studies on PBII treatment of light metals, which are of interest in the automotive and aerospace sectors because of their weight-saving character. However, often these materials suffer from poor tribological behavior and are often also temperature sensitive. PBII at a moderate temperature might improve the situation. In order to improve the performance of soft, light metal alloys such as aluminum, a relatively thick (i.e., tens of microns) load-supporting top layer is required which, however, may need a thin film for improving its friction properties. Matthews *et al*. combined microarc discharge oxidation (MDO) with PBII DLC on aluminum. They compared their tribological behavior in unlubricated pin-on-disc tests. The result shows that the combination of MDO and PBII gives enough strength under reduced friction to the soft aluminum to stand the test with a low friction coefficient; see Fig. 20.

Table 8
Critical galling loads for Staballoy AG17 stainless steel sliding against itself and other coated surfaces; data from ref. (37).

Coating	uncoated	TiN	CrN	PBII DLC
Critical galling load (N)	70	108	123	> 200
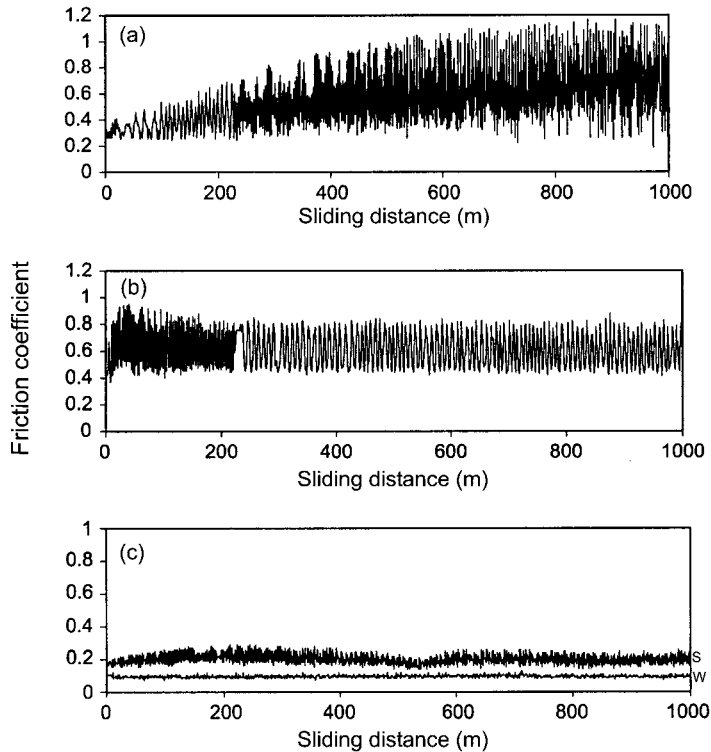
Fig. 20.   Influence of PBII DLC deposition on pin-on-disc sliding friction coefficients of MDO oxide coating on aluminium; (a) MDO aluminium against WC-Co ball, (b) MDO aluminium against SAE 52100 ball, (c) PBII DLC on MDO aluminium against both WC-Co (W) and SAE 52100 (S) balls; adapted from ref. 37.

4.3   *Gradient films on titanium alloys, aluminum alloys and steel*

Another approach to enhance adhesion and improve the tribological performance is to form gradient layers.

Ti-6Al-4V is a material which is well-known for its favorable mechanical properties, good corrosion resistance and biocompatibility. However, its tribological features are poor. In order to improve it, Xia *et al.* deposited a graded coating, composed of nitride and carbide of titanium, and a DLC film on top.[38] Samples of the titanium alloy were sputter-cleaned with argon ions and then treated by PBII in a two-step process, first with nitrogen at –60 kV then with a 1:1 gas mixture of acetylene and hydrogen. The conditions were –10 to –30 kV, 20 μs, and 100 Hz. The treatment time was 120 min. This led to a graded film composed of a carbon-, nitrogen-, titanium-, and oxygen-containing transition zone from the substrate to a DLC film on top. Figure 21 shows the C1s XPS lines of a sample treated at –20 kV. The C-C line gradually changes to the Ti-C line. The samples were subjected to wear tests. The counterbody was an identically treated Ti-6Al-4V ball, the load was 5 N, and the speed was 0.03 m s^{-1}. Figure 22 shows a comparison of the widths of the wear scars of the counterbody.
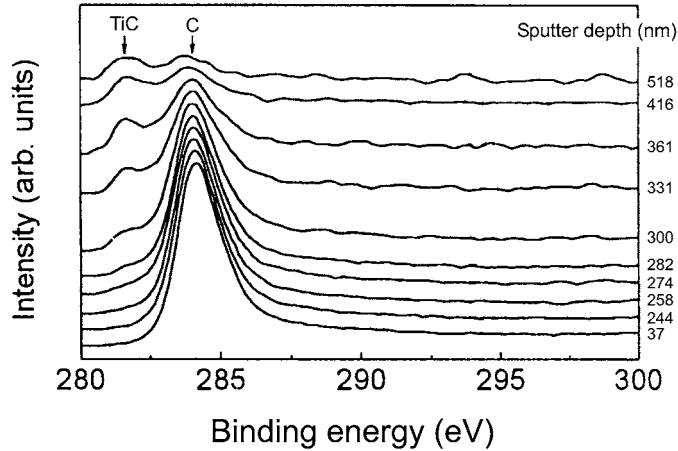
Fig. 21.   XPS C1s spectra as function of sputter depth; adapted from ref. 38.
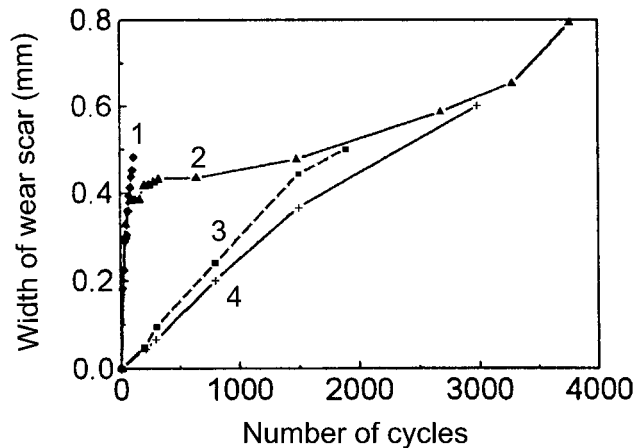
Fig. 22.   Width of wear scar of counterbody as function of number of wear cycles for different bias voltages; (1) unbiased (2) –30 kV, (3) –20 kV, (4) –10 kV; adapted from ref. 38.

The reduction in wear strongly depended an the PBII voltage. While the lower voltages gave similar good results, the films deposited at –30 kV failed earlier. The authors ascribe this to the internal stress of the top DLC film. This result shows that the PBII treatment considerably improves the tribological features, and that optimum process conditions with an intermediate pulse voltage exist.

Rather than forming the gradient nitride layer using the substrate itself, an additional metal can be deposited. Ma *et al.* modified 304 stainless steel by a combination of unbalanced magnetron sputtering and PBII.[39] They used a multistep procedure, starting with nitrogen implantation at –50 kV, followed by codeposition of titanium from the sputter source under concurrent implanation of nitrogen. Then, they deposited TiN at a substrate

bias voltage of –0.8 kV. In the third step, the gas was changed to methane and carbon was implanted, again at –50 kV. Eventually, the pulse voltage was decreased to –15 kV, and a DLC film was deposited with a $C_2H_2/H_2 = 3:1$ gas mixture. This resulted in a 200-nm-thick N/TiN/Ti (N,C)/DLC gradient film. AFM measurements gave a surface roughness of approximately 0.73 nm. The nanohardness was measured using a Berkovich indenter with a load from 1 to 10 mN. It gave a value of 19.1 GPa for the gradient film, as compared with the substrate with 3.2 GPa. In comparison, the nitrogen-implanted substrate was considerably softer; also, the N/TiN/Ti (N,C) gradient film was softer. The stability of a thin film also depends on its residual stress. In stress mesasurements, a N/TiN/Ti (N,C) layer and a DLC monolayer were compared with the N/TiN/Ti (N,C)/DLC film. Figure 23 shows the result. It turns out that the gradient films show a lower compressive stress level than the pure DLC film. With high hardness at a low stress level, the gradient film is superior to the N/TiN/Ti (N,C) film, which is softer, and the DLC film, which is slightly harder but shows a double stress level. The authors explain this with regard to a reduction in the thermal mismatch strain brought about by continuous changes in composition and microstructure from the top film to the substrate. In order to test the wear behavior, pin-on-disk measurements at a load of 50 mN and a relative humidity of 50% were carried out. For 30 min at a sliding speed of 1 mm/s, friction coefficient remained constant around an average value of 0.105.

The authors claim that the residual stress is much lower than values in the literature. The low compressive stress should yield strong adhesion between film and substrate. With these favorable tribological features, the coatings are suitable for space mechanic applications.

A similar technique has been used for 2024 aluminum alloy. Xia *et al*. combined N-PBII either with (a) C-PBII, (b) Ti-PBII/C-PBII or (c) (Ti,N)-PBII/C-PBII, and with (d) Ti-PBII/(Ti,N)-PBII /C-PBII[40]. N means nitrogen implantation, Ti means magnetron sputter deposition of a titanium film, either bombarded with argon ions (Ti-PBII) or nitrogen ions (Ti/N)-PBII. The pulse repetition rate was 80 Hz, and the pulse widths were 30 to 40 µs. For
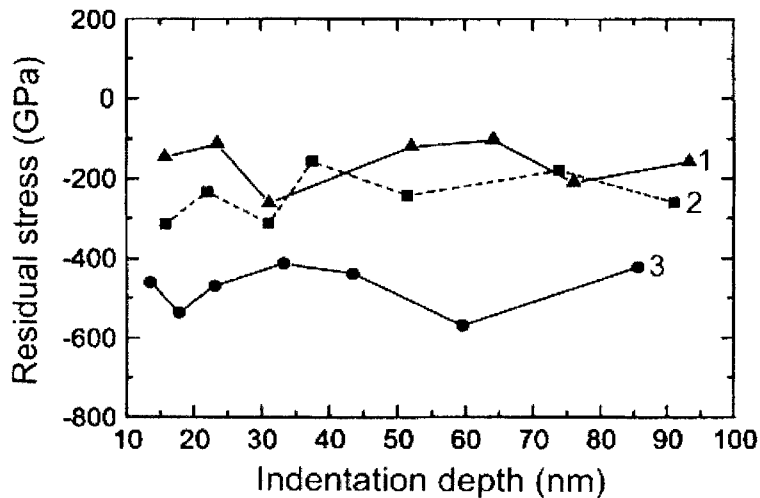
Fig. 23.   Variations in residual stresses as function of indentation depth; (1) N/TiN/Ti(N,C), (2) N/TiN/Ti(N,C)/DLC, (3) DLC; adpated from ref. 39.

nitrogen and titanium experiments, the bias voltage was high with –75 kV, and it was –10 kV for the deposition of DLC from an acetylene plasma. This treatment resulted in gradient films, corresponding to the according process, e.g., nitrogen implanted into the aluminum alloy, a nitrogen-containing titanium transition film, and a DLC film on top. Wear rate and friction were measured versus a 5 mm ball of hardened AISI 52100 steel at 40 rpm. The friction coefficients around 0.1 were very similar for all samples. This is due to the top DLC layer. However, the wear lives and rates differ.

Figure 24 shows a comparison of the wear rate of the different films. The best result is obtained for film (d) with the gradient layer of titanium and titanium/nitrogen.

This result demonstrates that a well-designed gradient film with transition layers from a metal substrate to the DLC film with a hard material interlayer can improve wear life greatly.

4.4. *Corrosion of DLC-coated nickel, steel and copper*

By far, the majority of the studies on PBII DLC films have been performed for tribological purposes. Only a few experiments have been carried out on corrosion. The studies of Chen *et al*.[10] and Baba and Hatada[26] on stainless steel have already been mentioned.

Lillard *et al*. investigated the corrosion protection effect of DLC on nickel.[41] They treated high-purity nickel with argon ions for cleaning, implanted carbon ions at –30 kV by PBII in a methane plasma, removed unwanted carbon deposits by argon sputter cleaning, and eventually deposited DLC from a RF acetylene plasma. The film thicknesses were 4 to 5 μm. The films were amorphous, had a density of 1.9 g/cm^3, and contained around 30 at% hydrogen. The hardness reached up to 12 GPa; the sp^3 content varied between 20 and 55%.

Electrochemical corrosion experiments were carried out in borate buffer at pH 7.2, 0.25 M sodium chloride at pH 7.0, and 1.0 M $NiCl_2$ at pH 6.1. Electrochemical impedance spectroscopy (EIS) was performed at the open circuit (corrosion) potential over the frequency range of 10^{-2} to 4×10^4 Hz. The potential scan rate in polarization measurements
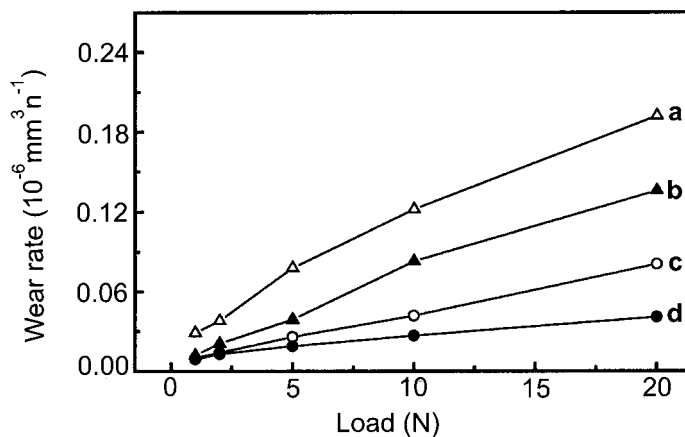
Fig. 24.   Wear rate as function of load for samples with different gradient layers, namely, N-PBII combined with (a) C-PBII, (b) Ti-PBII/C-PBII, (c) (Ti,N)-PBII/C-PBII, and (d) Ti-PBII/(Ti,N)-PBII /C-PBII; adapted from ref. 40.

was 0.1 mV/s.

Figure 25 shows the current/potential plots of nickel, uncoated and coated with DLC.[42] The corrosion potential is shifted to more noble values; the anodic dissolution currents are decreased by several orders of magnitude. This is an indication of a certain corrosion protection effect of the coating.

However, examination in a buffer solution showed that small defects were present in the film. These were presumably formed during the deposition process. When aggressive chloride was present, a rapid breakdown of the coating occurred at these pinholes. The initial step in this failure was the preferential dissolution of nickel from the carbon-implanted transition layer. The DLC coating with its large surface area acts as a cathode and increases the anodic reaction inside the pinhole. Nickel is dissolved and the coating is undermined. As a result, the coating around the pinholes breaks away.

Table 9 shows the data gained from EIS and SEM measurements. R_{corr} is the corrosion resistance of the pinholes; Θ is the fraction of the surface of the sample covered by them. When the immersion time in the corrosive medium is increased from 1 to 28 h, the corrosion resistance is deceased from 11 to 0.49 kΩ, while the defect area is increased from 0.003 to 0.08%.

The same group also investigated the corrosion behavior of the DLC-coated carbon steel C1018.[43] They carried out EIS measurements in ASTM artificial ocean water of pH 8.2 at
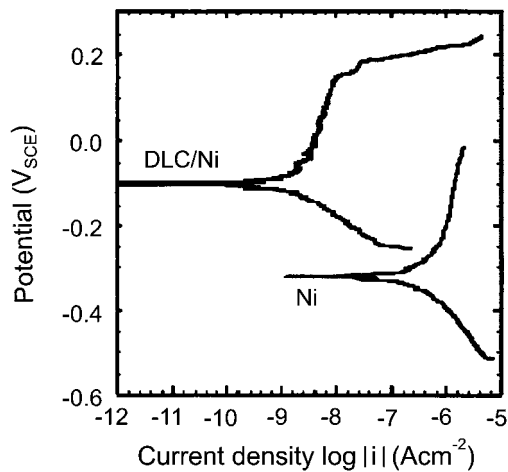
Fig. 25. Potentiodynamic polarization curves of nickel, uncoated and coated with DLC, adapted from ref. 42.

Table 9
Parameters of DLC-coated nickel, immersed for different periods of time in 0.25 M NaCl solution, from fitting of EIS data; R_{corr}: corrosion resistance of pinholes, Θ: percentage of area of surface covered with defects; data from ref. 41.

Immersion time (h)	R_{corr} (Ω)	Θ (%)
1	11400	0.003
24	2510	0.02
28	489	0.08

the open-circuit (corrosion) potential over the frequency range of 10^{-3} to 10^4 Hz.

Figure 26 shows the Bode magnitude and Bode phase plot of EIS measurements. The coating contains small pinholes that expose the carbon-implanted steel under the DLC. The figures show that for the first 20 days, only slight changes were observed. However, after 60 days of exposure, a large decrease in the low-frequency range of the Bode magnitude occurs, while an increase is observed in the Bode phase plot. This is an indication of coating failure. Inspection of the sample showed that parts of the coating had flaked off, and corrosion products were visible.

It can be concluded that corrosion started from preexisting defects, like in the case of nickel. The implanted carbon leads to galvanic corrosion. Some possibilities for improving the performance are as follows: reducing the number of pores in the DLC deposition process, and avoiding carbon implantation. However, from the latter arises the question of adherence, as it has been demonstrated earlier that the carbon-implant enhances adhesion.

Tonosaki *et al.* used a combined PBII technique to fabricate copper microtrench structures for micro-electro-mechanical systems (MEMS).[44] The application of such structures include microchannels or pumping devices for microfluids. For a good perfor-
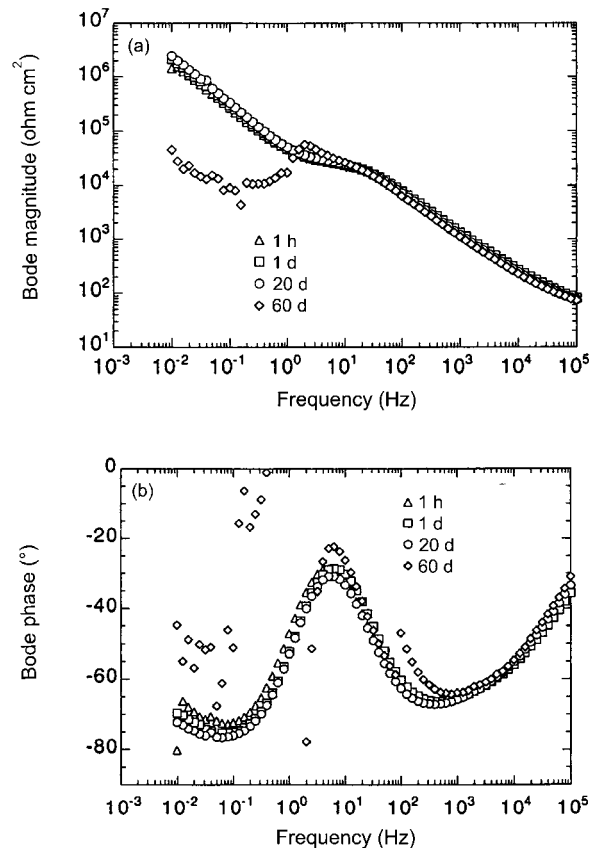
Fig. 26.   (a) Bode magnitude, and (b) Bode phase plot of DLC-coated C1018 steel in artificial seawater for different immersion times; adapted from ref. 43.

mance, they need corrosion-resistant hydrophilic surfaces. The authors prepared copper samples with trenches of 100 μm width and 40 μm depth by a conventional photochemical etching technique. DLC is a corrosion-resistant lubricant coating in water. However, a direct deposition of DLC onto copper did not lead to a good-quality coating. It tended to crack and showed poor adhesion. Therefore, a two-step process was carried out. First, the trenches were treated by PBII in an oxygen RF plasma. The voltage was –20 kV; the pulse duration was 20 μs. This led to an oxidation of the copper surface. On the oxide, DLC could be deposited with good quality from a methane plasma. The film thickness ranged between 100 and 300 nm. After the different treatments, the contact angle was measured. Table 10 shows a comparison. By means of the treatment, the trench surfaces become considerably more hydrophilic. The differently treated samples were subjected to a corrosion test in an environmental test chamber with 95% humidity and 80°C for a month. The untreated copper surface exhibited dark spots of corrosion products. The treated samples showed no damage.

These examples show that a corrosion protection effect can be achieved. However, care has to be taken in film deposition, particularly with respect to flaws.

5.   DLC Films on Polymers

PBII DLC flms were not only deposited onto metals but also on insulators, such as polymers. Watanabe *et al*. and Yoshida *et al*. formed DLC films on a polymer substrate.[44,45] This was poly-ethylene-terephthalate (PET), which is used in food technology for the storage of food and drinks. They used both CH_4 and C_2H_2, with voltages of –5 to –9 kV, a pulse length of 10 μs, a repetition rate of 300 Hz and a treatment time of 15 min. These are comparatively moderate conditions, suitable for treating polymers.

The use of CH_4 at a low gas pressure (5.4 Pa) resulted in CH_x ion implantation. In contrast, at a higher pressure (9.4 Pa), the deposition of DLC (a-C:H) was the main process. For C_2H_2, film deposition was always the dominant process, even at a low pressure (8.8 Pa).

When PET is used for food storage, one of the main issues is gas permeability. Oxygen is detrimental for food long-term storage. Another aspect is the adhesion and flexibility of the film. The authors measured the oxygen transmission rate (OTR) using a coulometric fuel cell sensor.

Table 11 shows the film thicknesses, the ratios of $sp^3/(sp^2 + CH)$ as obtained from Raman spectroscopy, and the OTRs. The bonding character of the films was mainly sp^2. The OTR was decreased by the DLC films by two orders of magnitude. It turned out that the deposited a-C:H films were better than those formed by ion implantation. SEM showed that the surface of the material has changed. The treated PET showed a smaller number of cracks.

This example shows the feasibility and beneficial effect of PBII DLC coating of polymers.

Table 10
Contact angles and appearance of treated copper samples; data from ref. 44.

Sample treatment	Contact angle (deg)	Appearance after corrosion test
Untreated	96	stained
Oxygen PBII	82	unchanged
DLC PBII	72	unchanged

Table 11

Thickness, bonding and oxygen transmission rate of DLC films deposited on PET; data from ref. 46.

Gas	Untreated	C_2H_2	CH_4	C_2H_2
Film thickness (nm)	—	110	(5–10) implanted	30
$sp^3/(sp^2+CH)$	—	0.06	0.11	0.17
OTR ($cm^3\ m^{-2}\ d^{-1}$) per unit thickness	63.3 ± 0.1	0.5 ± 0.01	1.3 ± 0.1	0.9 ± 0.01

6. Summary

For the deposition of thin films of diamond-like carbon with a certain amount of sp^3-bonds, a variety of techniques is available. Mostly, the processes are continuous, such as plasma-assisted chemical vapor deposition. The flow of the film-forming molecules or ions is usually constant over time, as well as the energy flow into the growing film. However, in most cases, when ions are used, their maximum energy is in the range of several keV. PBII differs from these in all aspects. The process is pulsed, leading to a pulsed energy input, and the ion energies can reach several 10 keV, typically from 10 to 60 keV. Apart from thin film deposition, the latter leads to ion beam mixing effects and to ion implantation. These strongly influence the film properties.

The balance between carbon ion implanation and DLC film deposition can be controlled by gas species, bias voltage, gas pressure, and length and repetition rate of the pulses. Gases with less carbon atoms, such as methane, lower gas pressure, higher bias voltage, longer pulses and higher repetition rates led to carbon implantation. Irradiation of the carbon film with high-current pulses or with high pulse repetition rates may lead to resputtering of the already deposited film with a reduced carbon film growth or even with a zero net deposition rate. This results in carbon ion implantation, forming a carbon-containing phase with the substrate material.

With the opposite choices, such as larger molecules with preformed C-C bonds, higher pressure, and lower bias voltages, DLC film deposition becomes the main process.

The tribological properties of the DLC films mainly depend on their hardness, smoothness, and adhesion. These are influenced by the stress state. As a general trend, it can be observed that an increase in gas pressure often decreases the obtained film hardness, but it increases the deposition rate. The decrease in hardness may come from the reduction in the ion energy, as the ions collide with gas molecules at high pressure. Here, PBII offers a means of counterbalancing this effect using higher pulse voltages. An optimum energy input into the growing film, mostly associated with a high content of sp^3-bonding, leads to maximum hardness.

A general problem of DLC films is that they often suffer from poor adhesion. The main cause for this is the presence of strong compressive residual stress which often reaches more than several GPa in DLC films and limits the available thickness. For an improved adhesion, PBII offers two ways. One is stress relief by energetic ion bombardment. Ion energy, pulse length, and pulse repetition rate can be used to control the stress level to a certain extent. The second method of enhancing adhesion is the formation of a gradient film between substrate and DLC film. For this purpose, several methods can be used. One is based on the use of two different gases, such as methane and acetylene or toluene. In the first step, methane is implanted and forms a carbide transition layer; in the second step, acetylene or toluene are

used to grow the DLC film. At a given bias voltage and gas pressure, methane-based ionic species have a higher kinetic energy per carbon atom than those of acetylene or toluene. This leads to implantation. Acetylene and toluene lead to DLC film formation. If no gas change is wanted, as a general rule, one finds better adhesion at higher bias voltages and lower gas pressure. These conditions lead to a certain degree of implantation that forms a carbide transition layer. In a more efficient way with respect to DLC film growth, the formation of a gradient implantation layer can be achieved by changing gas pressure and bias voltage. Initially, low pressure and high voltage are used, which lead to implantation. Then, voltage is decreased and pressure is increased. Both lead to a reduction in kinetic impact energy and, hence, to DLC formation. The lower kinetic energy reduces resputtering of the growing film with an increased growth rate. The higher pressure increases the film growth rate brought about by the larger number of species.

If PBII is combined with a metal deposition method such as sputtering or arc deposition, transition layers based on, e.g., titanium metal or titanium nitride or carbide can be formed. These also increase adhesion, act as a stable support for the DLC flms and improve the tribological performance.

One of the basic features of PBII is the possibilty of treating three-dimensional objects. However, here the problem of uniformity may arise. When a DLC film is being deposited from a plasma, such as in sputtering, vacuum arc deposition, and plasma CVD, the plasma is usually generated remote from the substrate. Often, there is a gradient along the substrate, particularly when it is three-dimensional. This effect is less distinct in PBII, but may still be found. However, different setups allow us to improve the homogeneity. In this case, the plasma has to be guided or enhanced at the substrate surface, e.g., by additional electrodes or electromangetic fields, such as in the case of cylinders or tubes, or a more uniform plasma has to be generated around the sample, e.g., when the substrate itself works as a RF antenna. This leads to a high degree of uniformity.

The examples and the observations of the relationship between PBII process parameters and the features of the DLC films show that PBII with its rich parameter matrix is a very effective method that allows us to deposit DLC films of excellent quality.

References

1) A. Anders (Ed.): *Handbook of Plasma Immersion Ion Implantation and Deposition* (John Wiley, New York, 2000).
2) J. R. Conrad and T. Castagna: Bull. Am. Phys. Soc. **31** (1986) 1479.
3) W. Ensinger: Nucl. Instrum. Methods Phys. Res. B **120** (1996) 270.
4) W. Ensinger: Surf. Coat. Technol. **100–101** (1998) 341.
5) W. Ensinger, J. Hartmann, J. Klein, P. Usedom, B. Stritzker and B. Rauschenbach: Mater. Res. Soc. Symp. Proc. **396** (1996) 521.
6) J. R. Conrad: J. Appl. Phys. **62** (1987) 777.
7) I. G. Brown, X. Godechot and K. M. Yu: Appl. Phys. Lett. **58** (1991) 1392.
8) I. G. Brown, A. Anders, S. Anders, M. R. Dickinson, I. C. Ivanov, R. A. McGill, X. Y. Yao and K. M. Yu: Nucl. Instrum. Methods Phys. Res. B **80/81** (1993) 1281.
9) J. Chen, J. Blanchard, J. R. Conrad and R. A. Dodd: Surf. Coat. Technol. **53** (1992) 267.
10) J. Chen, J. R. Conrad and R. A. Dodd: J. Mater. Eng. Perf. **2** (1993) 839.
11) J. Chen, J. R. Conrad and R. A. Dodd: J. Mater. Process. Technol. **49** (1995) 115.
12) C. P. Munson, R. J. Faehl, I. Henins, M. Nastasi, W. A. Reass, D. J. Rei, J. T. Scheuer, K. C. Walter and B. P. Wood: Surf. Coat. Technol. **84** (1996) 528.